Academic Journal of Science and Technology
ISSN: 2771-3032 | Vol. 14, No. 2, 2025

Shape Design and Analysis of Guide Pad for BTA Deep Hole Drilling Tool

Yazhou Feng[1], Xincheng Zhao[1], Zhanfeng Liu[2], Weiye Yang[1]

[1]School of Mechanical Engineering, Xi'an Shiyou University, Xi'an 710065, China
[2]Shanxi Shenkong Zhiyue Technology Co,Ltd., China

Abstract: According to the shape of the guide pad in the actual production, the force of the guide pad in the process of deep hole drilling is analyzed, and the results show that the force of the first guide pad is greater than that of the second guide pad. The reasonable shape of the guide pad is verified by displaying dynamic simulation and test by ABAQUS software. The results show that when the arc guide pad is used, the contact stress with the workpiece is small, the cutting formed is an ideal shape, and the dimensional accuracy, surface roughness and straightness of the parts meet the machining requirements.

Keywords: BTA deep hole drilling tool, guide pad, shape.

1. Introduction

With the progressive advancement of science and technology, deep-hole components have found extensive applications across various industries. The BTA deep hole drilling process has been empirically validated as one of the most cost-effective manufacturing techniques for achieving superior geometrical characteristics, including high aspect ratios, exceptional parallelism, precise straightness, optimal roundness, and controlled surface finish parameters99[1] .BTA deep hole machining has become a widely used deep hole machining technology because of its wide processing range, good machining quality and stable machining performance[2]. The BTA deep hole drilling tool consists of multiple asymmetrical cutting edges and guide pads. The guide pad is a vital component of the BTA deep hole drilling tool, serving critical functions such as centering and self-guidance during the drilling process[3]. Through systematic experimentation and analysis, Sakuma.K, Katsuki.A, Taguchi.K[4]have identified that the guide pad assembly generates a dual mechanical interaction with the machined surface, characterized by both compressive stress distribution and controlled abrasive action. This tribological phenomenon induces a surface refinement process that significantly improves the surface finish quality, effectively reducing the surface roughness of the internal cylindrical bore through mechanical polishing and micro-level surface modification. Experiments conducted by Fu.Hongge,Zhan Liying[5] revealed that an overly long guide pad intensifies the torsional deformation of the drill bit. Cuiping Zhao[6]proposed replacing the edges of the front extrusion section of the guide pad with arcs. This modification not only achieves better surface roughness but also reduces the wear of the guide pad during the machining process. Zhao Bo and Huazhen Dan[7] established an extrusion model for the guide pad and discovered that the shape of the front section of the guide pad significantly influences both the wear of the guide pad and the quality of hole machining. Wang. Z. M and Su. D[8]investigated the machining techniques, geometric parameters of tools, and processing parameters for deep-hole parts. Through the optimization of cutting parameters, they successfully attained superior dimensional precision and surface smoothness in the processed deep holes.

In practical machining, guide pads of different shapes typically exert corresponding influences on the drilling process. This paper establishes contact models between two distinctively shaped BTA deep hole drill guide pads and the hole wall. Utilizing Abaqus for simulation, the study captures the variations in contact stress on the guide pads, leading to the selection of the optimal guide pad design. Subsequently, drilling experiments employing the selected guide pad are conducted to validate the finite element simulation results.

2. BTA Deep Hole Drilling Tool Force Analysis

(1) The Workpiece Analysis

The workpiece is a kind of high temperature nickel base alloy GH4169 with slender shaft structure, and its structure is show in Figure 1.The outer diameter of the workpiece is Ø82mm and the length is 2145mm. The workpiece has an inner diameter of Ø70mm at both ends, a deep hole of length 24mm, and a deep hole of inner diameter of Ø66.5mm and length of 2037mmin the middle. Its chemical composition is shown in Table 1 below:

Table 1. Chemical composition of alloy GH4169

Chemical element	Ni	Cr	Fe	Nb	Mo	Ti	Other
Mass fraction (%)	52.5	18.2	18.2	5.2	2.6	1.1	2.2

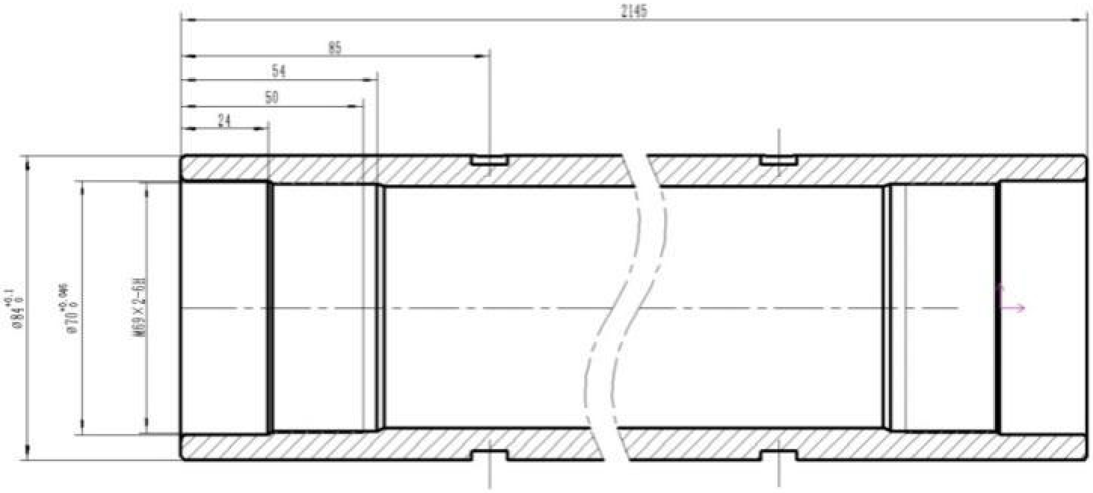

Figure 1. Structure of the workpiece

It can be seen from the workpiece structure diagram that the workpiece is a through-hole structure, so whether the through-hole machining accuracy meets the requirements determines whether the whole part is qualified or not. In order to meet the design requirements of the workpiece, the through-hole machining is usually divided into two steps, that is, the through-hole structure with diameter Ø65mm is drilled first and then the hole is drawn. This research specifically focuses on the machining characteristics and process optimization of through-hole structures with a nominal diameter of Ø65mm.

(2) Analysis of working state of guide pad

The BTA deep hole drilling tool usually consists of several blades, several guide pads and a tool body, and its structure is shown in Figure 2. The first guide pad is close to the center cutting tooth, and the second guide pad is close to the intermediate cutting tooth. The two guide pads play the role of guiding and grinding the inner wall of the machined hole in the machining, and the guide pad is the key to produce the workpiece that meets the design precision. The wear of the guide pad will cause the guide pad to be unable to transfer the cutting force to the hole wall, thus causing the axis line of the machined hole to deflect, and the wear of the guide pad can be reflected by the contact stress, usually the greater the contact stress with the hole wall, the faster and deeper the wear of the guide pad.

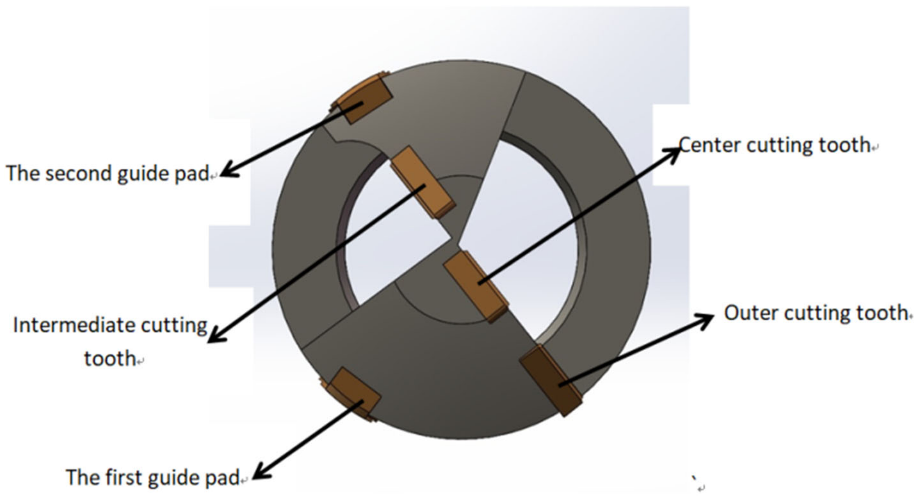

Figure 2. Working status of guide pad

Figure 3 shows the simplified mechanical model of the guide pad of the BTA deep hole drill. The positive pressure of guide pad 1 is N_1, and the friction force is F_{f1}; the positive pressure of guide pad 2 is N_2 and the friction force is F_{f2}. The resultant forces of the two guide pads are F_1 and F_2. F is the combined force of radial cutting force F_x and tangential cutting force F_y, and the angle is λ. The angle between the guide pad 1 and the positive direction of the X axis is α_1, and the angle between the guide pad 2 and the positive direction of the X axis is α_2.

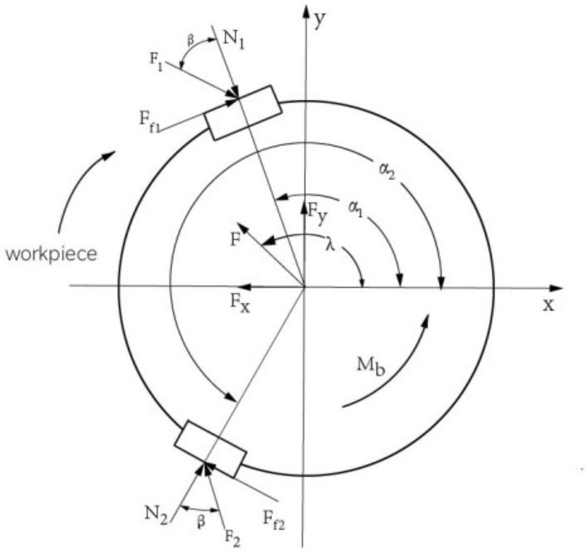

Figure 3. The force acting on the guide pad

It can be obtained from the figure:

$$\begin{cases} \overline{F_1} = \overline{N_1} + \mu\overline{F_{f1}} \\ \overline{F_2} = \overline{N_2} + \mu\overline{F_{f2}} \end{cases} \quad (1)$$

In the formula, the μ friction coefficient and the force are all average.

The balance of radial force can be obtained:

$\sum F_x = 0$:$F\cos\lambda - F_1\cos(\alpha_1+\beta) + F_2\cos(\alpha_2+\beta) = 0$

$\sum F_y = 0$:$-F\sin\lambda + F_1\cos(\alpha_1+\beta) - F_2\cos(\alpha_2+\beta) = 0$

In the formula, the angle between the β positive pressure and the resultant force of the guide pad.

The calculation of the above two formulas can be obtained:

$$F_1 = \frac{F\sin(\lambda-\alpha_1-\beta)}{\sin(\alpha_2-\alpha_1)} \quad (2)$$

$$F_2 = \frac{F\sin(\lambda-\alpha_2-\beta)}{\sin(\alpha_2-\alpha_1)} \quad (3)$$

The following conclusions can be drawn from formulas (2) and (3):

$|\alpha_2-\alpha_1| = 90°$, the values of F_1 and F_2 are minimum. When λ = 90 °, the drilling process is unbalanced.

$90° \le |\alpha_2-\alpha_1| \le 180°$, drilling is a state of equilibrium.

$|\alpha_2-\alpha_1| > 180°$, that's not going to happen.

BTA deep hole drilling tool is mainly affected by friction force, extrusion force and radial cutting force. The force is shown in Figure 4.

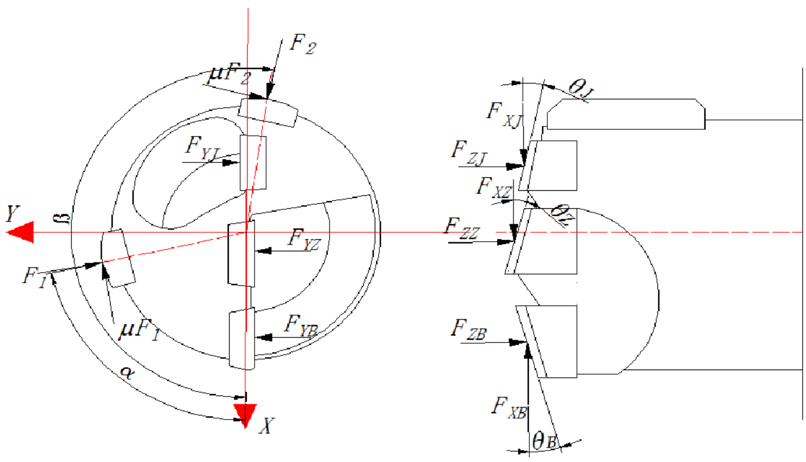

Figure 4. Force diagram of BTA deep hole drilling tool

$$F_{XZ} = F_{ZZ}\cdot\tan\theta_Z, F_{XJ} = F_{ZJ}\cdot\tan\theta_J, F_{XB} = F_{ZB}\cdot\tan\theta_B \quad (4)$$

$$F_{YZ} = \frac{2a\times M}{R^2},\ F_{YJ} = \frac{2b\times M}{R^2},\ F_{YB} = \frac{2C\times M}{R^2} \quad (5)$$

$$F_{ZZ} = a\times\frac{T}{R},\quad F_{ZJ} = b\times\frac{T}{R},\ F_{ZB} = c\times\frac{T}{R} \quad (6)$$

In the formula, F_{XZ}, F_{XJ} and F_{XB} are the radial forces of three cutting teeth, F_{YZ}, F_{YJ} and F_{YB} are the tangential forces of three cutting teeth, and F_{ZZ}, F_{ZJ} and F_{ZB} are the axial forces of three cutting teeth, and their units are all N. A, b, c are the cutting widths of three cutting teeth, in units of mm. θ_Z, θ_J, θ_B are the cutting angle of cutting teeth, unit is °

The formula for calculating the axial resultant force T and M torque is as follows:

$$T = b\tan\lambda\,(\sigma\cdot VB + 2f\cdot\cos\lambda\cdot\tau + HB\cdot r\cdot\sin 45^{\circ} \quad (7)$$

$$M = 1.8\times10^{-4}\times K_s\times f\times D^2 \quad (8)$$

In the formula, F is the axial force of cutting teeth, unit: n; λ is approach angle, unit is °; σ is yield strength, unit MPa; f is feed, unit: mm/r; τ is shear stress, unit: MPa; HB is Brinell hardness; r is tool tip arc radius, unit: mm; M is torque, unit: N·mm; K_s is high temperature nickel base alloy GH4169 specific cutting force is 3320N.

3. Modeling and Simulation of BTA Deep Hole drilling tool

(1) Material constitutive model

The cutting process is the plastic deformation of metal, which usually occurs under the conditions of high temperature, high pressure, large stress and large strain rate, so an appropriate constitutive model is a necessary prerequisite to ensure the accuracy of finite element simulation. In this paper, Johnson-Cook constitutive model is selected, and its expression is as follows:

$$\sigma_{JC} = [A + B(\varepsilon)^n]\left[1 + C\ln\left(\frac{\dot{\varepsilon}}{\dot{\varepsilon_0}}\right)\right]\left[1 - \left(\frac{T - T_0}{T_M - T_0}\right)^m\right]$$

In the formula: σ_{JC} is the equivalent flow stress of the material; A is the yield stress of the material; B is the strain hardening coefficient; C is the strain sensitivity coefficient; n is the strain hardening index; m is the temperature sensitivity coefficient; T is the deformation temperature; T_m is the melting temperature; ε is the equivalent plastic strain; $\dot{\varepsilon}$ is the equivalent plastic strain rate; $\dot{\varepsilon_0}$ is the reference value of the strain rate.

The parameters of the GH4169 constitutive model are shown in Table 2 below. The tool selects YG8 cemented carbide with CBN coating, and its material properties with the workpiece are shown in Table 3 below.

Table 2. Parameters of Johnson-Cook constitutive model for high temperature nickel base alloy GH4169

Model parameters	A(MPa)	B(MPa)	C	n	m
Value	450	1700	0.017	0.65	1.3

Table 3. Material properties of workpiece and tool material

	Elastic(MPa)	Poisson	Density(tone/mm^3)
workpiece	1.13×10^5	0.3	4.43×10^{-9}
tool	7×10^5	0.2	3.48×10^{-9}

(2) Establishment of geometric model

The geometric dimensions of the clamp blade and tool body used in the simulation are selected as reference Sandvik drilling samples, and their geometric parameters are shown in Table 4 below. The shape of the guide pad is modeled according to two commonly used shapes in actual production, and its geometric shape is shown in Figure 5.

Table 4. Geometric parameters of cutter teeth

	Tool approach angle(°)	Tool cutting angle(°)	Width of cutting tool(mm)
Outer cutting tooth	14	76	13
Center cutting tooth	18	72	9.12
Intermediate cutting tooth	15	75	11.12

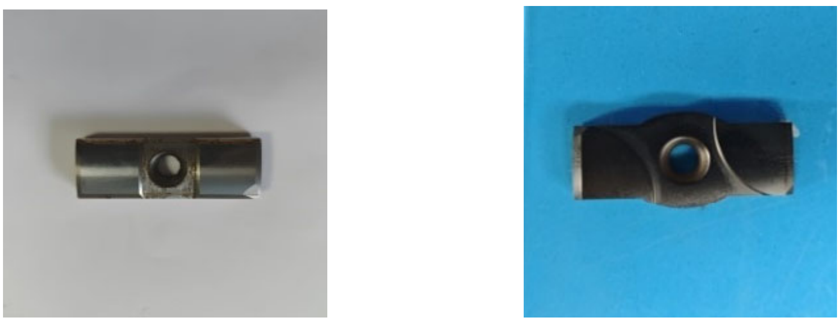

(a) Bond guide pad (b) Arc shape guide pad

Figure 5. Two different guide pad shapes

According to the selected size, the 3-D model of BTA deep hole drilling tool is established, and the details are ignored to save simulation time. The simplified three-dimensional model is shown in Figure 6. This part of the simulation also needs to establish a circular workpiece, assemble it with the tool, and then import it into the Abaqus software. The result is shown in Figure 7:

Figure 6. Simplified 3D model of BTA deep hole drilling tool

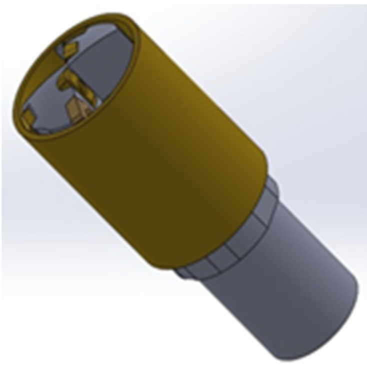

Figure 7. Assembly model of tool and workpiece

(2) Simulation parameter setting

The grid between the tool and the workpiece is shown in Figure 8. According to the actual situation, the part is set to the contact layer and the base layer, and the upper and lower size ratio is 2:1. The type of workpiece grid is C3D8R, which is set to hourglass control, integral reduction and unit deletion to ensure simulation efficiency, and tool grid adopts S4R and is set to rigid body.

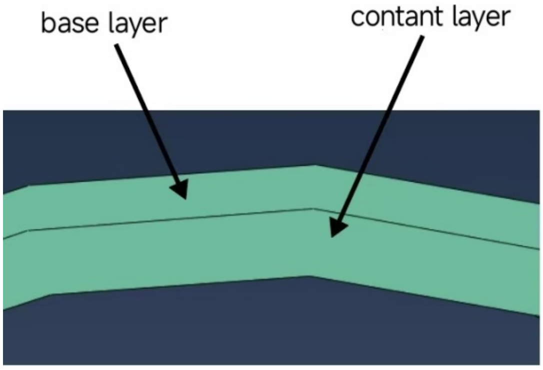

Figure 8. Mesh of workpiece

The outside of the workpiece base layer is completely fixed, and the rotational speed 20.4rad/s and the feed speed 0.814mm/s are applied to the center point of the bottom surface of the tool. The cutting force calculated by equations (4), (5), (6), (7) and (8) is simplified to a concentrated force applied on the center point of the cutting edge, and the cutting edge is coupled with the central point. The result is shown in Figure 9.

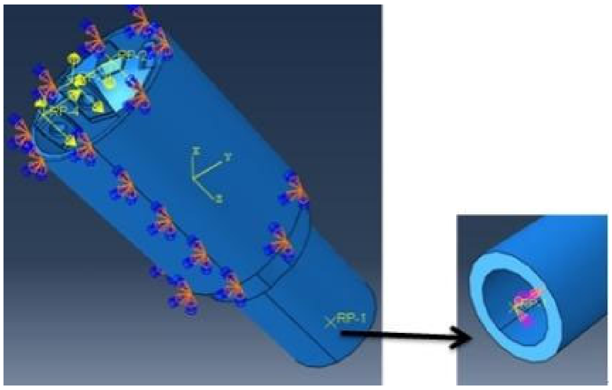

Figure 9. Load and boundary conditions applied

4. Simulation results and experimental verification

(1) Simulation analysis results

A conclusion can be drawn from Figure 10:

1. From the analysis of the contact stress distribution, the shape of the guide pad has nothing to do with the contact stress distribution. The contact stress distribution of the first guide pad is more uniform than that of the second guide pad, indicating that the contact area between the first guide pad and the inner wall of the workpiece is larger.

2. From the analysis of the contact stress, the contact stress of the first guide pad is greater than that of the second guide pad. This is because in the working process, the tangential component mainly acts on the first guide pad, and the radial component mainly acts on the second guide pad, and the tangential component is larger than the radial component. This verifies the calculation and analysis in the first chapter of this paper.

3. From the analysis of the shape of the guide pad, the contact stress of the arc guide pad in the machining process is less than that of the key guide pad. This situation is beneficial to processing.

(2) Analysis of test conditions and results

The test adopts the deep hole drilling and boring machine modified by the CW6163D lathe shown in Figure 11, and its spindle speed range: 110r/min - 1100r/min, drill pipe length 3000mm, can complete the deep hole machining of the part. The machine clamp BTA deep hole drilling tool with arc guide pad is shown in Figure 12, and the selection of process parameters is the same as the simulation setting.

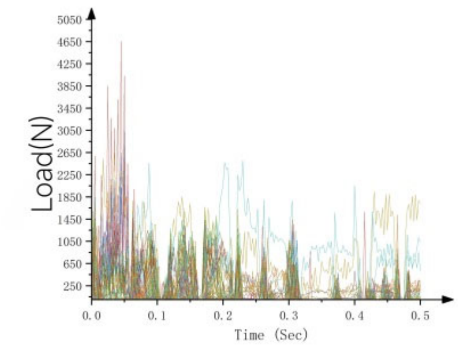

(a)The first bond guide pad

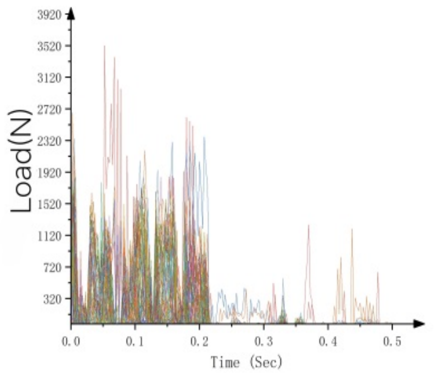

(b)The second bond guide pad

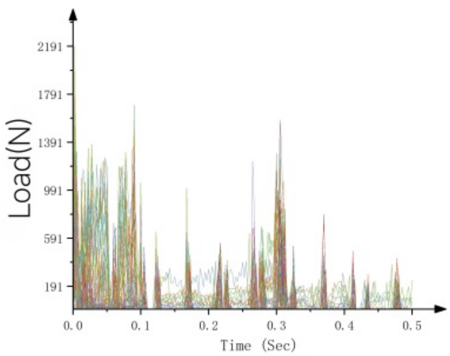

(c) The first Arc shape guide pad

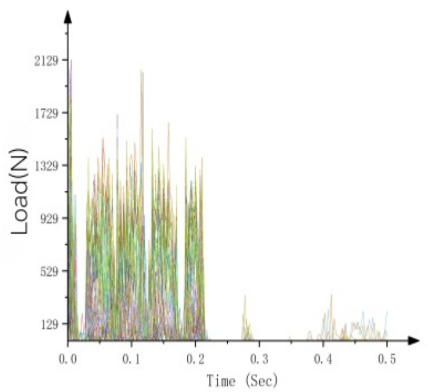

(d) The second Arc shape guide pad

Figure 10. Contact stress of two different shapes of guide pads

Figure 11. CW6163D deep hole drilling machine and workpiece

Figure 12. Cutting tools used for testing

The condition of the machined guide pad is shown in Figure 13 and Figure 14.

1. The wear edge of the first guide pad is flat, and the wear edge of the second guide pad has more protuberances. This situation shows that the contact stress distribution of the first guide pad is more uniform than that of the second guide pad.

2. It can be seen that the wear area of the first guide pad is large and there is a deeper wear depth in the red ring; the wear area of the second guide pad is smaller, and the wear of each position is smooth and does not appear a deeper wear depth.

The status of the machined guide pads is consistent with the simulation results, which shows that the contact stress simulation of guide pads with different shapes has a certain reference value.

Figure 13. Wear state of the first guide pad

Figure 14. Wear state of the second guide pad

(3) Chip morphology analysis

The three-point fixed circle composed of the edge structure of the auxiliary cutting edge of the guide pad and the outer tooth can ensure that the tool is not prone to deflection and vibration in the drilling process, so that it has good drilling stability. The wear of the guide pad will lead to the failure of three-point circle setting and the aggravation of cutting tooth wear, which will eventually lead to the workpiece being unable to meet the machining requirements and then scrapped. Therefore, the tool wear state at a certain time can reflect the working state of the guide pad at this time. Because deep hole drilling is carried out in high temperature, high pressure and closed state, the tool wear state is not easy to be observed directly. In actual production, the degree of tool wear is often judged by observing the chip shape.

The cutting speed of the outer cutting tooth is the highest, and most of the chip bending radius is spiral chip, and its evolution process is shown in Figure 15. The cutting speed of the intermediate cutting tooth is between the outer cutting tooth and the center cutting tooth, and the chip produced by the intermediate tooth is in a long spiral shape, and the evolution process is shown in Figure 16. The cutting speed of the center cutting tooth is the smallest, and the resulting chip is in the shape of a pagoda. Figure 17 shows its evolution state.

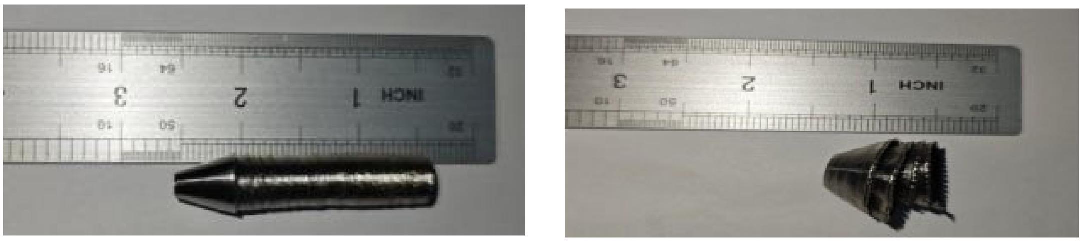

(a) At the beginning (b) In the drilling process

Figure 15. Chip morphology formed by outer cutting tooth

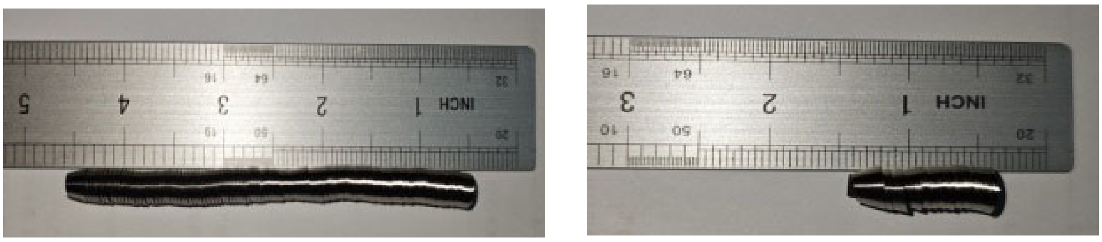

(a) At the beginning (b) In the drilling process

Figure 16. Chip morphology formed by intermediate cutting tooth

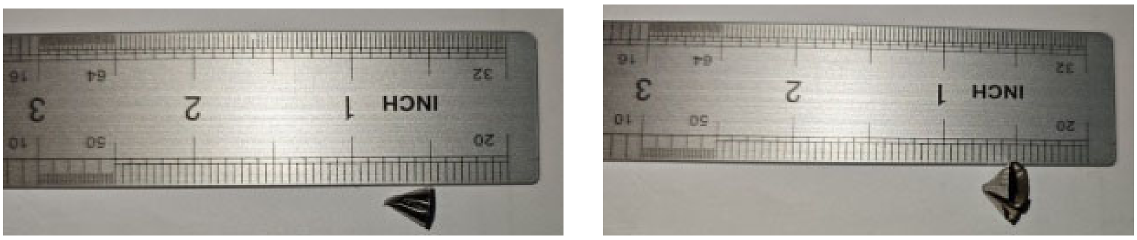

(a) At the beginning (b) In the drilling process

Figure 17. Chip morphology formed by center cutting tooth

In the process of machining, the chip shape is ideal and there is no obvious edge burr, the chip discharge condition is good, the chip plugging phenomenon does not occur, the drill pipe vibrates smoothly, and the tool feed state is good.

(3) Analysis of workpiece processing result

The drilled workpiece of high temperature nickel base alloy GH4169 is shown in Figure 18. After testing, the dimensional accuracy, surface roughness and straightness meet the machining requirements.

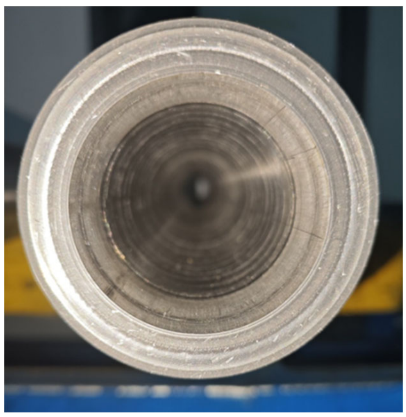

Figure 18. Inner hole of workpiece after actual machining

5. Conclusion

1.Firstly, the force of the guide pad is analyzed, and the results show that the contact stress of the first guide pad is much larger than that of the second guide pad. The conclusions are verified by follow-up simulation and machining experiments.

2. The drilling process is simulated by using ABAQUS simulation software. After processing the simulation results, it is found that the contact stress of the first guide pad is larger and the stress distribution is uniform, and the contact stress of the arc guide pad is less than that of the key guide pad.

3. The arc guide pad is selected for drilling experiment. The formed chips are all in ideal shape, which can be discharged smoothly from the arbor without chip plugging, the drilling is smooth, and the machining accuracy of the workpiece meets the machining requirements.

Acknowledgements

This research was funded by the Shaanxi Provincial Key Research(2022QCY-LL-45) and Natural Science Basic Research Program of Shaanxi(2023-JC-YB-475) and Xi'an Key Research(23ZCKCGZH0010).

References

[1] R., Richardson, and, R., & Bhatti. (2001). A review of research into the role of guide pads in BTA deep-hole machining. Journal of Materials Processing Technology, 110(1), 61–69.

[2] Chunrui Li.(2008).Characteristics study of deep hole drilling tool system. Xi'an University of Technology

[3] Sakuma K, Taguchi K, Katsuki A, elc. Self-Guiding Action of Deep-Hole-Drilling Tools. CIRP Annals, 1981, 30(1): 311～315

[4] Fu, H., & Zhang, L. (n.d.). The model and experimental study for vibration control in Deep-hole Boring. 2011 Second International Conference on Mechanic Automation and Control Engineering.

[5] Cuiping Zhao. (1995). Relation between shape number of BTA cutter guide pad and machining quality. Journal of ZHENGZHOU University (03), 62-66

[6] Bo Zhao, Huazhen Dan. (1993). Relationship between Guide block and hole machining quality. Modern Manufacturing Engineering (04), 7-9.

[7] Wang Z M, Ezugwu E O, Su D. Advances in the precision machining of small deep holes. Journal of Materials Processing Technology, 1997, 68(3): 257～261

[8] Yanjun Hu., & Zhanli Wang,el c. Machining simulation during metal milling based on DEFORM-3D. Manufacturing Technology & Machine Tool (01), 94-99.